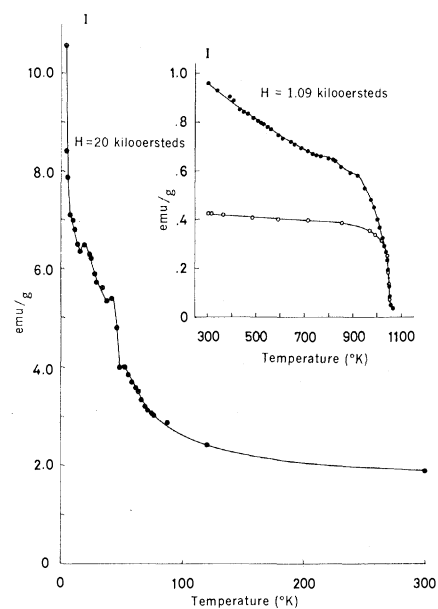


Fig. 1 (left). Magnetization ( $I$ ) versus temperature ( $T$ ) for lunar crystalline rock 10024, 22. Solid circles are observed values; unbroken lines are the simulated curve and the basic curves of the dependences of magnetization of  $\text{Fe}^{2+}$ ,  $\text{FeTiO}_3$  on temperature; the broken line is the basic dependence of the Fe particle on temperature.

Fig. 2 (right). Magnetization ( $I$ ) versus temperature ( $T$ ) for lunar fines 10084,89. Solid circles are observed values before heating to  $800^\circ\text{C}$ ; open circles are observed values after heating to  $800^\circ\text{C}$ .



oersted $^{-1}$ . If the observed natural remanent magnetization is assumed to be the thermoremanent magnetization, the magnetic field during the cooling period must be about  $2600 \gamma$ . This value seems hardly probable. Moreover, the heterogeneity of the remanent magnetization is incompatible with the homogeneity of the thermoremanent magnetization. The saturated magnetization and the saturated isothermal remanent magnetization of the ferromagnetic component of this rock at room temperature are  $1.55 \times 10^{-1}$  emu/g and  $1.52 \times 10^{-3}$  emu/g, respectively; these values are about  $2 \times 10^1$  and  $2 \times 10^2$  times as large, respectively, as the natural remanent magnetization.

Although the cause of the observed natural remanent magnetization has not yet been identified, it seems likely that the remanent magnetization might be caused by (i) an instantaneous local magnetic field generated by some kind of lightning, (ii) the piezomagnetic effect caused by meteorite impacts in the presence of a weak solar wind magnetic field, or (iii) a simple heterogeneous distribution of fine single-domain particles of metallic irons.

The same sequence of analyses was used for lunar fines (10084,89). Both x-ray microprobe and magnetic analyses have shown that magnetic minerals in the lunar fines are basically the same as in the lunar crystalline rock 10024,22; that is, that magnetic minerals in the fines are paramagnetic pyroxenes, antiferromagnetic Fe pyroxenes, antiferromagnetic ilmenites, and metallic irons

(see Fig. 2). However, the saturation magnetization of the ferromagnetic component (metallic iron) of the lunar fines at room temperature amounts to 1.17 emu/g, which is about 7.5 times as large as the same magnetic parameter of the crystalline rock. The curve of magnetization versus temperature in Fig. 2 also indicates that the abundance of antiferromagnetic ilmenite is less and the abundance of antiferromagnetic and paramagnetic pyroxenes is more in the lunar fines than in the crystalline rock.

Analyses of the magnetization versus magnetic field curves at various temperatures have shown that about 20 percent of metallic iron in the crystalline rock and about 50 percent of metallic iron in the fines is superparamagnetic and in the form of very fine grains, which are less than  $100 \text{ \AA}$  in mean diameter and which are superparamagnetic at temperatures above room temperature. These fine grains seem to be easily oxidized to become wüstite ( $\text{FeO}$ ) at high temperatures, even in a high vacuum chamber. The remaining metallic irons are considered to be of fairly large size, and their magnetization curve is subjected to the shape demagnetiza-

tion effect. For instance, five pieces of 92 spherules separated from 150 mg of the lunar fines are iron spherules with diameters that range from 20 to  $100 \mu\text{m}$  and with Fe contents that range from 85 to 90 percent ( $\pm 5$  percent).

T. NAGATA, Y. ISHIKAWA  
H. KINOSHITA, M. KONO, Y. SYONO  
University of Tokyo, Tokyo, Japan

R. M. FISHER  
U.S. Steel Corporation Research Center,  
New York 10006

#### References and Notes

1. T. Nagata, *Rock Magnetism* (Maruzen, Tokyo, 1961), pp. 76-78.
  2. A. Sawaoka, S. Miyahara, S. Akimoto, *J. Phys. Soc. Japan* **25**, 1253 (1968).
  3. Y. Ishikawa and S. Akimoto, *ibid.* **13**, 1298 (1958); J. J. Stückler, S. Kern, A. Wold, G. S. Heller, *Phys. Rev.* **164**, 765 (1967).
  4. R. M. Bozorth, *Ferromagnetism* (Van Nostrand, Princeton, N.J., 1951), pp. 53-55 and 160-180.
- 4 January 1970

## Magnetic Resonance Properties of Some Lunar Material

**Abstract.** Paramagnetic resonance spectra of Apollo 11 fines and rocks were measured at 9 and 35 gigahertz and at  $4^\circ$ ,  $80^\circ$ , and  $300^\circ\text{K}$ . At both frequencies the material has an intense absorption at  $g = 2$ , with a line width of  $\sim 950$  gauss. Fe ions with strong exchange interactions produce this resonance. A comparison of the resonance absorption due to  $\text{Fe}^{3+}$  showed that the energy of the crystal field interaction was  $\sim 0.1$  per centimeter.  $\text{Mn}^{2+}$  was identified in several samples, and an absorption at  $g = 1.89$  was tentatively attributed to  $\text{Ti}^{3+}$ . The nuclear magnetic resonance spectra of  $^{27}\text{Al}$  had a distribution of asymmetry parameters  $\eta$  ranging from 0.25 to 0.75 and had nuclear quadrupole coupling constants  $e^2qQ/h$  of approximately 3 megahertz.

Elements present in lunar material (Apollo 11) with the highest relative abundance, which would be expected to produce electron paramagnetic reso-

nance absorption (EPR), are Ti, Cr, Mn, and Fe ( $I$ ).  $\text{Ti}^{3+}$ ,  $\text{Mn}^{2+}$ , and  $\text{Fe}^{3+}$  have the highest probability of being detected (2). Exposure of rocks and

minerals to energetic photons and particles can introduce paramagnetic defect states, the concentration of which may be a measure of the integrated flux of radiation (3). The valence states of ions such as  $\text{Fe}^{3+}$  and  $\text{Mn}^{2+}$  may also be altered by radiation (4). The characteristics of nuclear magnetic resonance (NMR) spectra are determined by interactions between nuclear magnetic moments and nearby electrons localized on the nucleus, on surrounding atoms, and in a metal by the conduction electrons (5). In lunar material (Apollo 11) the nuclei that are present in amounts sufficient to be detected by usual experimental techniques (5) are  $^1\text{H}$ ,  $^{23}\text{Na}$ ,  $^{27}\text{Al}$ , and  $^{29}\text{Si}$ .

Samples from rocks 10065 and 10062 and from fines were encapsulated in containers (3), which were either sealed with a cap or sealed to an ion pump in the vacuum chamber (F201) in the Lunar Receiving Laboratory. EPR and NMR measurements could be made with the material in the container, and samples were therefore relatively uncontaminated by terrestrial atmosphere. The pressure in containers with attached ion pumps has been  $\leq 10^{-8}$  mm Hg since their removal from F201. Samples from rocks 10046, 10047, and 10057 encapsulated in air and from 10046 and 10005 encapsulated in  $\text{N}_2$  were received. EPR and NMR measurements were repeated on 10062 and 10065 samples after exposure first to  $\text{N}_2$  and then to air. Magnetic separation of fines failed, owing to the attraction of most of the particles by the magnet. Subsequently, mineral separations were made in air based on gross visual differences seen through a microscope with  $\times 30$  magnification. Part of sample 10047-49 was also separated in this fashion into three components: (i) fragments with an amber color in transmission, (ii) lustrous, opaque, black fragments with conchoidal surfaces, and (iii) colorless, white, or transparent fragments.

EPR measurements were made at 9 and 35 GHz at 4°, 80°, and 300°K. Resonance lines are designated by  $g = h\nu/\beta H$ , where  $H$  is the value of the magnetic field at which  $dI/dH$ , the derivative of the absorption, changes sign,  $\nu$  is the spectrometer frequency,  $\beta$  is the Bohr magneton, and  $h$  is Planck's constant. NMR measurements were made over a range of resonant frequencies from 8 to 16 MHz by means of a Varian wide-line NMR spectrometer with a Varian "proton free" probe and a time-averaging computer.

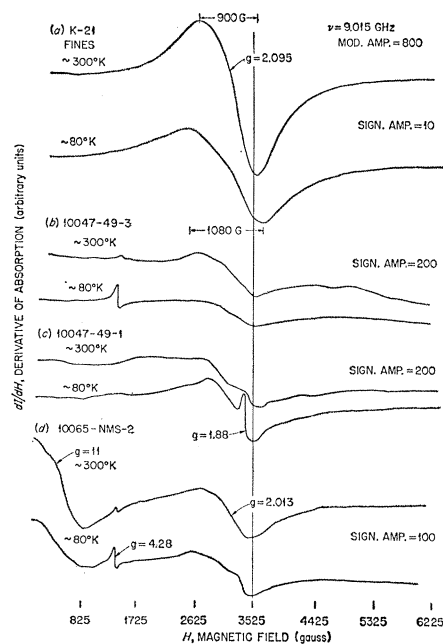


Fig. 1. Effect of temperatures on resonance spectra of several lunar samples.

$^1\text{H}$  was not detectable in the probe and container for a 90-trace readout from the time-averaging computer for a 500-second trace time.

A spectrum characteristic of as-received fines and of 10065 (encapsulated in F201, exposed to  $\text{N}_2$  and then to air) and many other rock fragments is shown in Fig. 1a. For this line  $2.01 < g < 2.11$  and the width  $\Delta H$  of the line measured between the two inflection points of the derivative curve is  $900 \leq \Delta H \leq 980$

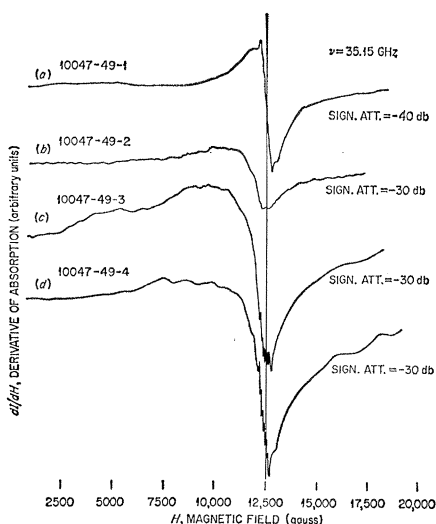


Fig. 2. Electron paramagnetic resonance spectra of mineral separates from rock 10047-49. (a) Amber, transparent,  $\sim 3$   $\text{mm}^3$  (sample 1); (b) lustrous, black, opaque, conchoidal surfaces,  $\sim 3$   $\text{mm}^3$  (sample 2); (c) colorless, white, transparent [ $\sim 10$  percent (A) and (B) material],  $3$   $\text{mm}^3$  (sample 3).

gauss at both 9 and 35 GHz when measured at room temperature. At 9 GHz,  $\Delta H$  increased from 900 to 1080 gauss when the temperature was decreased from 300° to 80°K (compare the two curves in Fig. 1a). There was also a twofold decrease in peak-to-peak height. Use of the equation  $I \sim \Delta H^2 h_{pp}$ , where  $h_{pp}$  is peak-to-peak height, gives the intensity of the absorption at 80°K as  $\sim 12$  percent less than at 300°K. At 4°K it was not possible to make direct comparisons of intensity with the measurements at 80° or 300°K. On the basis of a comparison of spectrometer sensitivities at the two temperatures, the intensity of the detected resonance was at least 100 times less than the resonance detected at 300°K.

Resonance spectra at 9 GHz of two fractions of 10047-49 are shown in Fig. 1 (c, b). At 300°K the  $g = 2.1$  resonance in 10047-49-2 and 10047-49-3 decreased in intensity with decreasing temperature, whereas in 10047-49-1 the absorption in this region of  $g$  value increased. These samples differed in other respects. A resonance in 10047-49-3 at  $g = 4.28$ , quite weak at 300°K, showed a fourfold increase in intensity at 80°K. This resonance was not detected in either 10047-49-1 or 49-2. Resonance absorption at  $g = 1.89$  in 10047-49-1, with a temperature dependence similar to the  $g = 4.28$  resonance in 10047-49-3, was not detected in either 10047-49-3 or 49-2.

A nonmagnetic piece of 10065 has a spectrum (Fig. 1d) that is quite different, except in the region of  $g = 2$ , from the spectrum of the magnetic fraction. The resonance at  $g = 2$  was similar in width, shape, and temperature dependence to the resonance in Fig. 1a. There was an intense absorption at  $g = 11$  and a weak one at  $g = 4.28$  at 300°K. At 80°K the resonance at  $g = 11$  decreased twofold in intensity and the resonance at  $g = 4.28$  increased fourfold. The change in the shape of the absorption at  $g = 1.89$  with decrease in temperature, which can be seen by comparing the two curves in Fig. 1d, is probably due to a resonance similar to the one in 10047-49-1.

The spectra of the three fractions of 10047-49 measured at 35 GHz and 300°K are all characterized by relatively intense absorption in the region of  $g = 2$ . Sample 10047-49-1 has an almost symmetric absorption in this region (Fig. 2a). Although not well resolved in the figure, the central part contains six equally spaced lines with a spacing

of 90 gauss and  $g = 2.00$ . This six-component spectrum has better resolution in the curves for 49-3 and the powder (Fig. 2, c and d). It was not detected in 49-2. The broad asymmetric shape of the  $g = 2.1$  absorption in 49-3 is similar to the resonance in amber-colored fragments separated from the fines sample (for example, amber spheres).

All the described resonances had an intensity that was proportionate to incident microwave power and shapes that were independent of power when it was  $< 0.3$  watt.

Room temperature NMR spectra of  $^{27}\text{Al}$  ( $I = 5/2$ ) from a sample of 10062 and of 10065 were recorded in the dispersion mode. Two of the spectra are shown in Fig. 3 (b and c) with the spectrum of the probe, sample container, and  $^{27}\text{Al}$  in  $\text{AlCl}_3$ , which was used as a reference for  $\nu_0$ , in Fig. 3a. Line shapes were due to second-order quadrupole broadened ( $1/2 \leftrightarrow -1/2$ ) transitions (5) with a distribution of nuclear quadrupole coupling constants and of asymmetry parameters. These spectra are characterized by nuclear quadrupole coupling constants of several megahertz. An estimate of the asymmetry parameters  $\eta$  was obtained by comparison with  $^{27}\text{Al}$  resonance from powdered samples of microcline ( $\eta = 0.21$ ,  $e^2qQ/h = 3.22$  MHz), and albite ( $\eta = 0.62$ ,  $e^2qQ/h = 3.29$  MHz) (6) and was found to range from 0.25 to 0.75. Spectra of  $^1\text{H}$  from 10062 and 10065 and from 5 grams of fines were not obtained in reproducible form for integration times  $> 30$  hours. Spectra of  $^{23}\text{Na}$ ,  $^{29}\text{Si}$ , and  $^{47,49}\text{Ti}$  were not detected for integration times  $\sim 10$  hours.

The most probable source of the intense resonance that is characteristic of the fines and breccia samples is  $\text{Fe}^{3+}$ , but other types of resonance from Fe (such as ferromagnetic resonance) may also contribute to the resonance absorption. The frequency-independent  $g$  value and the temperature dependence of width and intensity of this characteristic line are evidence that these properties are determined by strong magnetic interactions between the paramagnetic ions. Such interactions could occur in metallic particles of iron whose diameter is smaller than a domain (superparamagnetism) (7) or in regions of an oxide of iron where there is a high concentration of paramagnetic  $\text{Fe}^{3+}$ . No resonance absorption would be expected in pure  $\text{FeO}$  under the condition of these experiments, but partly reduced  $\text{Fe}_2\text{O}_3$

has an intense resonance with characteristics similar to the lunar material resonance (Fig. 1a).

$\text{Fe}^{3+}$  in crystal fields of symmetry lower than cubic, in which the energy of interaction of the  $d^5$  electrons with the crystal field is of the same order of magnitude as  $h\nu$ , where  $\nu$  is the frequency of measurement, may have strong resonance absorptions at  $g \sim 10$ ,  $g \sim 6$ ,  $g = 4.28$ , and  $g \sim 0.8$  (8) depending on the symmetry of the crystal field. Absorption at  $g \sim 10$ ,  $g = 6$ , and  $g = 4.28$  has been observed in many compounds (2) and in silicate glasses (9). On the basis of these data and analyses, the  $g = 11$ ,  $g = 4.28$  absorptions shown in Fig. 1 are due to  $\text{Fe}^{3+}$ . The increase in absorption at high field observed in 10047-49-3 may be due to absorption from  $\text{Fe}^{3+}$ , which in some crystal fields would have an absorption peak at  $g \sim 0.8$ . The decrease in intensity of the absorption at  $g = 11$  in 10065-NMS-2 and at high fields in 10047-49-3 is consistent with this assignment. Since these absorptions may occur in an excited electronic state (depending on the nature of the crystal field interactions), a decrease in temperature decreases the population of electrons in the states with a resultant decrease in absorption. Measurements at 35 GHz show that most of the resonance absorption is in the neighborhood of  $g = 2$  and that none is observed at  $g \sim 11$  or  $g \sim 4.28$ . Hence, we can conclude that the crystal field interactions are much less than  $h\nu$ , when  $\nu = 35$  GHz ( $1.2 \text{ cm}^{-1}$ ).

$\text{Cr}^{3+}$  and  $\text{Ti}^{3+}$  in various crystals have resonance absorptions at  $g < 2.0$  (2).  $\text{Cr}^{3+}$  is usually observed at  $300^\circ\text{K}$ , whereas  $\text{Ti}^{3+}$  is usually observed only at temperatures  $\leq 80^\circ\text{K}$ . On the basis of the relatively high abundance of Ti as compared with Cr in lunar material (Apollo 11) and the temperature dependence of the  $g = 1.89$  absorption, we tentatively attribute this absorption to  $\text{Ti}^{3+}$ . The congruence of spacing and  $g$  value of the six-line set in 10047-49-1, 49-3, and powder with the six hyperfine lines of the ( $1/2 \leftrightarrow -1/2$ ) electronic transition of  $\text{Mn}^{2+}$  in many silicate minerals (4) is positive identification of  $\text{Mn}^{2+}$  in these samples. This assignment is also supported by the relative abundance of Mn ( $\sim 0.2$  percent). The width and shape of these lines are similar to those of  $\text{Mn}^{2+}$  in amorphous compounds, such as tektites (4).

EPR absorption due to singly charged oxygen vacancies has been found in

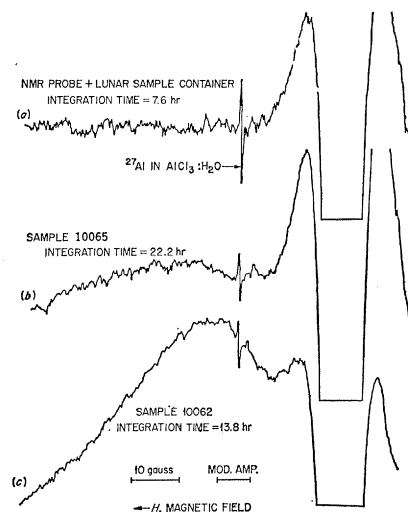


Fig. 3. Nuclear magnetic resonance spectra of  $^{27}\text{Al}$  in lunar material (Apollo 11) at  $\nu_0 = 16$  MHz recorded in the dispersion mode. The two samples whose measurements are shown in (a) and (b) were of approximately equal volume.

several silicate minerals after irradiation with energetic protons (3). Lunar surface material, if exposed to a sufficiently large flux of solar protons, particularly energetic flare protons, might be expected to exhibit a similar absorption. A flux of  $\sim 10^{16} \text{ cm}^{-2}$  of 40-Mev cyclotron protons at  $T \sim 100^\circ\text{C}$  during irradiation is sufficient for the production of enough centers in  $\sim 3 \text{ mm}^3$  of sample of a mineral to be easily detected. In none of the white and colorless transparent fragments separated from our fines sample, or in 10047-49-3 or 10047-49-1, with the possible exception of one piece, was this absorption observed. In view of (i) the small distance of penetration of protons ( $\sim 3 \text{ mm}$  for 40-Mev protons incident on olivine), (ii) the relatively low flux per year of protons with energy  $\geq 10$  Mev (of the order of  $10^{10} \text{ cm}^{-2}/\text{year}$ ) (10), (iii) the relatively short exposure time reported for lunar material (Apollo 11) ( $\sim 10^7$  to  $\sim 10^8$  years), and (iv) the small probability of obtaining material from within 0.5 cm of the surface due to mixing during collection and return, this negative result is not unexpected.

R. A. WEEKS, A. CHATELAIN  
J. L. KOLOPUS

Solid State Division,  
Oak Ridge National Laboratory,  
Oak Ridge, Tennessee 37830

D. KLINE  
State University of New York,  
Albany 12203

J. G. CASTLE  
University of Alabama,  
Huntsville 35807

## References and Notes

1. Lunar Sample Preliminary Examination Team, *Science* 165, 1211 (1969).
2. W. Law and E. L. Offenbacher, *Solid State Phys.* 17, 136 (1965).
3. R. A. Weeks and J. L. Kolopus, Paramagnetic Resonance Spectra of Some Silicate Minerals, "Semi-Annual Progress Report for Period Ending June 30, 1968," (ORNL-CF-69-3-5, contract NASA-MSC-76458).
4. R. A. Weeks and J. L. Kolopus, Paramagnetic Resonance Spectra of Some Silicate Minerals, "Semi-Annual Progress Report for Period Ending June 30, 1968," (ORNL-CF-68-8-38, contract NASA-MSC 76458).
5. A. Abragam, *The Principles of Nuclear Magnetism* (Oxford Univ. Press, London, 1963); C. P. Slichter, *Principles of Magnetic Resonance* (Harper & Row, New York, 1963).
6. P. Hartmann, thesis, University of Zurich, Switzerland (1963).
7. C. P. Bean and J. D. Livingston, *J. Appl. Phys. Suppl.* 30, 1205 (1959).
8. H. H. Wickman, thesis, University of California (UCRL Rep. 11538).
9. E. Lell, N. J. Kreidl, J. R. Hensler, *Progr. Ceram. Sci.* 4, 59 (1966).
10. E. J. Zeller, L. B. Ronca, P. W. Levy, *J. Geophys. Res.* 71, 4855 (1966).
11. Research sponsored by the U. S. Atomic Energy Commission under contract with Union Carbide Corporation and by NASA contract MSC-T-76458. We thank H. S. Story (State University of New York at Albany) for his comments on the NMR results, M. M. Abraham (Oak Ridge National Laboratory) for his comments on the EPR results, S. Hafner (University of Chicago) for his comments on the NMR measurements, and Orson Anderson (Lamont-Doherty Geological Observatory) for the loan of his ~5-gram sample of fines.

4 January 1970

## Optical and High-Frequency Electrical Properties of the Lunar Sample

*Abstract. Reflectivity and polarization laws for the powder sample and its spectrum are close to the mean for the lunar maria. Solid samples show a marked absorption feature at 1 micron. The low albedo appears to be due to a surface coating on dust grains rather than to volume absorption. The high-frequency electrical properties resemble those of a fine powder made from typical dense terrestrial rocks and are consistent with previous estimates from ground-based radar observations. The differential mass spectrum is almost constant from 100-micron particles down to 0.1-micron particles; most particles are smaller than 0.3 micron. Their shapes disclose a variety of processes of generation.*

Lunar dust and rock chip samples have been analyzed in the lunar laboratory of the Cornell Center for Radiophysics and Space Research; our concern has been with the optical and electrical properties of the sample and their relation to those known for the lunar surface as a whole, and with the questions surrounding the origin of the lunar dust. Four salient points have emerged.

1) The optical scattering law and polarization properties of a surface of lunar dust generally correspond closely to these properties as observed for the moon as a whole. The rock chip sample shows a strong absorption feature at 1  $\mu\text{m}$  which is not prominent in the lunar scattered light. It is probable, therefore, that most of the lunar surface is covered with a material similar to the powder that was investigated.

2) The dielectric constant is within the range that had been estimated for the moon as a whole by radar methods.

3) The particle size distribution indicates that the differential mass spectrum as a function of radius is almost constant from 100  $\mu\text{m}$  down to 1000  $\text{\AA}$ . The shapes of the particles indicate a variety of sources. Some have the sharp edges that are characteristic of

fracture; others are rounded, indicating processes of melting or condensation. Some cannot readily be attributed to either of these mechanisms.

4) The darkness of the lunar dust is mainly due to dark surface deposits on the grains, probably metallic, rather than to absorptivity of the bulk material.

The optical scattering law as a function of phase angle and the optical polarization law were measured with

the same instrument that had been used for measuring many sample powders in the past and in the same manner (1). The lunar powder proved to resemble, both in appearance and in the measured optical properties, the lunar maria as observed from the earth and the terrestrial powders previously proposed (1) as being most closely representative of the moon. These powders also proved to be similar under optical microscope examination. The particle size was similar, the great majority of the particles being less than 10  $\mu\text{m}$  in diameter. The adhesion of the small particles to each other indeed created the "dendritic growth" appearance under the microscope that has been given the name "fairy castles." It appears that the large part of the pronounced lunar opposition effect—that is, the brightness surge toward zero phase—can be attributed to the shadows cast by this lacy surface structure.

Figures 1 and 2 summarize the optical properties of the Apollo 11 samples. Each data point represents the mean of several observations of different portions of a sample, and the measurements repeated very well. In Fig. 1 the photometric phase function of the lunar dust sample is generally steeper than the mean lunar case (1) for phase angles less than 15°, but the difference is very small. The curve for polarization plotted against phase angle (Fig. 1) also demonstrates the similarity of the dust sample to the moon as a whole, but, again, there are minor differences; the crossover from negative to positive polarization occurs at a lower phase angle, and polarization in the positive branch is greater.

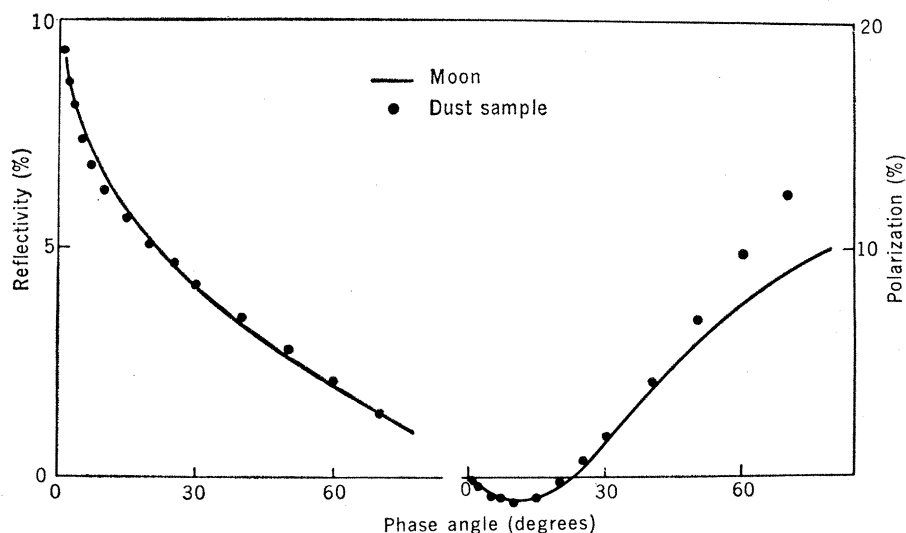


Fig. 1. The dependence of reflectivity and polarization on phase angle at wavelength of 5600  $\text{\AA}$  and at normal viewing. [Curve for the moon from Watson and Danielson (3)]